BIOCHEMISTRY
including biophysical chemistry & molecular biology

Article

pubs.acs.org/biochemistry

NMR and Fluorescence Studies of Drug Binding to the First Nucleotide Binding Domain of SUR2A

Jorge P. López-Alonso,[†,‡,§] Elvin D. de Araujo,[†,‡] and Voula Kanelis*[,†,‡,§]

[†]Department of Chemical and Physical Sciences, University of Toronto Mississauga, 3359 Mississauga Road, Mississauga, Ontario, Canada L5L 1C6

[‡]Department of Chemistry, University of Toronto, 80 St. George Street, Toronto, Ontario, Canada M5S 3H6

[§]Department of Cell and Systems Biology, University of Toronto, 25 Harbord Street, Toronto, Ontario, Canada M5S 3G5

Supporting Information

ABSTRACT: ATP sensitive potassium (K_{ATP}) channels are composed of four copies of a pore-forming inward rectifying potassium channel (Kir6.1 or Kir6.2) and four copies of a sulfonylurea receptor (SUR1, SUR2A, or SUR2B) that surround the pore. SUR proteins are members of the ATP-binding cassette (ABC) superfamily of proteins. Binding of MgATP at the SUR nucleotide binding domains (NBDs) results in NBD dimerization, and hydrolysis of MgATP at the NBDs leads to channel opening. The SUR proteins also mediate interactions with K_{ATP} channel openers (KCOs) that activate the channel, with KCO binding and/or activation involving residues in the transmembrane helices and cytoplasmic loops of the SUR proteins. Because the cytoplasmic loops make extensive interactions with the NBDs, we hypothesized that the NBDs may also be involved in KCO binding. Here, we report nuclear magnetic resonance (NMR) spectroscopy studies that demonstrate a specific interaction of the KCO pinacidil with the first nucleotide binding domain (NBD1) from SUR2A, the regulatory SUR protein in cardiac K_{ATP} channels. Intrinsic tryptophan fluorescence titrations also demonstrate binding of pinacidil to SUR2A NBD1, and fluorescent nucleotide binding studies show that pinacidil binding increases the affinity of SUR2A NBD1 for ATP. In contrast, the KCO diazoxide does not interact with SUR2A NBD1 under the same conditions. NMR relaxation experiments and size exclusion chromatography indicate that SUR2A NBD1 is monomeric under the conditions used in drug binding studies. These studies identify additional binding sites for commonly used KCOs and provide a foundation for testing binding of drugs to the SUR NBDs.

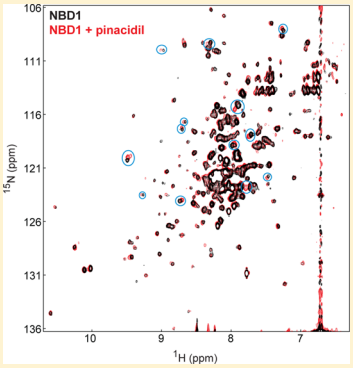

ATP sensitive potassium (K_{ATP}) channels are non-voltage-dependent, potassium selective channels present in many tissues including the brain, pancreas, smooth muscle, and heart.[1] Because gating of K_{ATP} channels depends on cellular concentrations of ATP and ADP, K_{ATP} channels couple the metabolic state of the cell to membrane potential[2] and thus play crucial roles in many biological processes. In the heart, K_{ATP} channels are normally closed, but they open in response to various forms of stress including ischemia, physical exertion, and hypertension.[3] Opening of cardiac K_{ATP} channels contributes to increases in K^+ influx and shortening of action potentials, which may protect the heart against arrhythmias.[1] Furthermore, activation of K_{ATP} channels in the heart during ischemia renders the heart more resistant to subsequent ischemic events, which minimizes cardiac damage.[1,3,4]

K_{ATP} channels are composed of four copies of a pore-forming inward rectifying potassium channel (Kir6.2 or Kir6.1) and four copies of a sulfonylurea receptor (SUR1, SUR2A or SUR2B) that surround the pore.[5] Different combinations of Kir6.x and SUR proteins form K_{ATP} channels in different tissues that have different nucleotide and pharmacological sensitivities.[6−11] The SUR proteins are members of the ubiquitous ATP-binding cassette superfamily of proteins and consist, at minimum, of two membrane spanning domains (MSD1 and MSD2) and two cytoplasmic nucleotide binding domains (NBD1 and NBD2)[12] (Figure 1A,B). In the SUR proteins and related ABC transporters, these domains are arranged in the sequence MSD1-NBD1-MSD2-NBD2. The transmembrane helices in the MSDs extend into the cytoplasm and are connected by short loops,[13−15] with short segments in the connecting loops, known as coupling helices,[16] contacting the NBDs (Figure 1A,B). MgATP binding causes dimerization of NBD1 with NBD2, which dissociate upon ATP hydrolysis.[17] In addition to the minimum ABC protein structure, the SUR proteins contain another MSD (MSD0) that is linked to the N terminus of MSD1 by the cytoplasmic L0 linker.[18−21] ATP binding, in the absence of Mg^{2+}, at the Kir6.x proteins (Figure 1C) results in K_{ATP} channel inhibition, whereas MgATP binding and hydrolysis at the SUR NBDs result in channel opening.[22]

The SUR proteins are also sites of binding of K_{ATP} channel openers (KCOs).[23] These structurally diverse drugs are used in the treatment of disorders such as hypertension, angina, and

Received: July 28, 2012
Revised: October 16, 2012
Published: October 18, 2012

dx.doi.org/10.1021/bi301019e | *Biochemistry* 2012, 51, 9211−9222

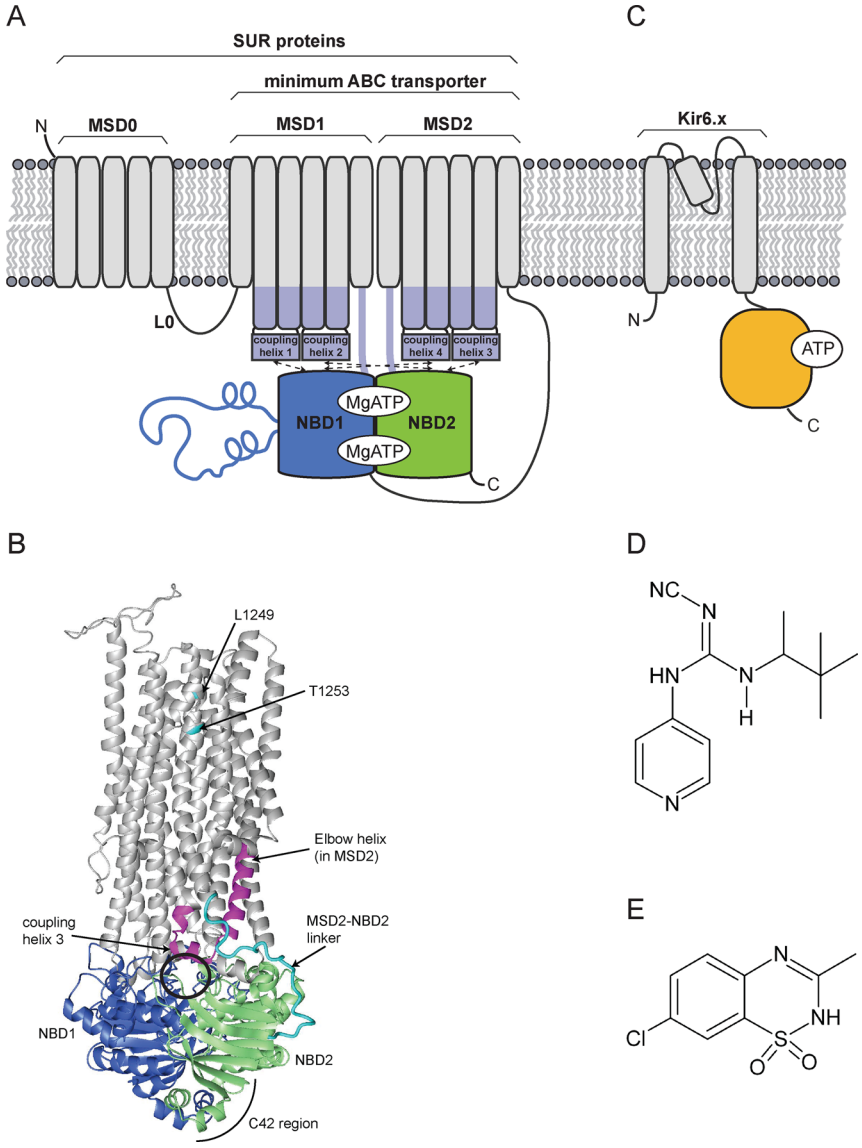

Figure 1. Structures of SUR and Kir6.x proteins, and common K_{ATP} channel openers. (A) Schematic diagram of a SUR protein. The transmembrane helices in each membrane-spanning domain (MSD0, MSD1, and MSD2) of the SUR protein are shown in gray. The L0 linker connects MSD0 to the minimum ABC transporter structure.[18−21] Binding of MgATP at NBD1 (blue) and NBD2 (green) results in NBD1/NBD2 dimerization.[17] Hydrolysis of MgATP to MgADP at the NBD2 composite site results in dissociation of the dimer (not shown). NBD1 contains a large disordered loop represented by the blue curve.[38] Cytoplasmic extensions of the transmembrane helices in MSD1 and MSD2 are shown in light purple. Coupling helices, also shown in light purple and labeled, connect the helical extensions and contact the NBDs (black, dashed arrows).[13−16] (B) Ribbon diagram of the homology model of SUR2A with NBD1 and NBD2 colored in blue and green, respectively. The MSDs are primarily colored in gray, with the exception of part of the cytoplasmic loop between TM helices 13 and 14, that includes coupling helix 3 and is important for pinacidil binding and activation of K_{ATP} channels,[36] which is magenta. The MSD2-NBD2 linker and residues L1249 and T1253 in TM helix 17, also important for K_{ATP} channel activation,[37] are in cyan. The C42 region in NBD2 is indicated. A solid black circle shows the location of a possible drug binding interface.[6] (C) Schematic diagram of Kir6.x proteins. The two transmembrane helices and the pore helix embedded in the membrane of the Kir6.2 subunit are colored in gray. The C-terminal domain, which binds ATP in absence of Mg^{2+}, is colored in yellow.[76] In the K_{ATP} channel, the SUR and Kir6.x proteins interact via the transmembrane helices of Kir6.x and MSD0 of the SUR protein.[5,18,77] (D and E) Chemical structures of the K_{ATP} channel openers (D) pinacidil and (E) diazoxide.

ischemic heart disease, and are also used for cardioprotection in surgery.[4,24,25] Figure 1, panels D and E show the structures of two commonly studied KCOs, pinacidil and diazoxide, respectively. K_{ATP} channels from different tissues display varying sensitivities to these KCOs, and the differential responses of K_{ATP} channels to the drugs are attributed to the specific SUR protein.[6,26] For example, pancreatic K_{ATP} channels, which contain four copies of SUR1, are activated by diazoxide and to a small extent by pinacidil.[27−29] In contrast, the SUR2A-containing cardiac K_{ATP} channels are activated by pinacidil and generally not by diazoxide,[28−32] except under specific conditions (see below). Finally, K_{ATP} channels in smooth muscle, which contain SUR2B, are activated by both pinacidil and diazoxide.[30,33] In addition to differences in activation by different KCOs, specific SUR proteins in K_{ATP} channels differ in the degree to which their response to the drugs is modulated by nucleotides. For example, diazoxide activates SUR1- and SUR2B-containing K_{ATP} channels in the

dx.doi.org/10.1021/bi301019e | *Biochemistry* 2012, 51, 9211−9222

presence of both MgATP and MgADP, while only MgADP and not MgATP supports diazoxide activation of SUR2A-containing cardiac K_{ATP} channels.[34]

The differential activation of K_{ATP} channels containing either SUR1 or SUR2 isoforms by pinacidil and diazoxide has been exploited to identify regions of the SUR proteins involved in KCO binding and/or mediation of the effects of the drugs. Binding studies using [^{3}H]P1075, an analogue of pinacidil, and electrophysiological experiments on SUR1-SUR2A chimeras originally localized the pinacidil binding site to a segment of SUR2A comprised of transmembrane (TM) helices 12−17.[35] Additional [^{3}H]P1075 binding and channel activation studies narrowed the site of action to residues T1059-L1087 (rat SUR2A numbering) and R1218-N1320.[36] Residues T1059-L1087 encompass the cytoplasmic loop between TM helices 13 and 14 (Figure 1B, magenta) and include coupling helix 3 that contacts both NBD1 and NBD2. Residues R1218-N1320 form TM helix 17 and the MSD2-NBD2 linker (Figure 1B, cyan), plus the first β-strand of NBD2 (Figure 1B, green). Channel activation studies using mutations in which L1249 and T1253 in TM helix 17 in SUR2A were changed to Thr and Met, the corresponding residues in SUR1, respectively, identified these residues as critical for KCO-mediated activation of K_{ATP} channels.[37] Thus from these data, two different regions in the SUR protein appear to be involved in KCO binding and channel activation.

The C-terminal 42 residues in the SUR protein, known as the C42 region, define a third region as being involved in KCO binding and KCO-mediated activation. K_{ATP} channels containing either SUR2A or SUR2B, which differ only in the composition of the C42 region but are otherwise identical, display different affinities for various KCOs, with SUR2B-containing channels having a higher affinity for the drugs than SUR2A-containing channels.[23] Further, a chimera comprising the SUR2 core structure and the C42 region of SUR1, which is similar in sequence to that of SUR2B, binds P1075, pinacidil, and diazoxide with an affinity similar to SUR2B, consistent with the involvement of the C42 region in drug binding.[23] The C42 region is part of the NBD2 domain,[38] and homology models of SUR2A NBD2 and SUR2B NBD2,[39] based on the structure of the histidine permease NBD,[40] suggest interactions of the C42 region with the ATP-binding site in NBD2. Homology models of the minimum ABC structure of SUR2A (Figure 1B), as well as structures of ABC transporters Sav1866,[14] MsbA,[15] and murine P-glycoprotein,[13] which were not available at the time the C42 experiments were done, demonstrate that the C42 region is not located near the TM helices or coupling helix 3. However, the C42 region is at the NBD1/NBD2 dimer interface and hence may affect drug binding because of its influence on NBD1/NBD2 dimerization. The apparent discrepancy resulting from identification of three distant regions in SUR2A in pinacidil binding and activation may be due to pinacidil inducing structural changes in the protein, which are in turn necessary for channel activation. Some of the regions identified by mutation studies may be involved in drug binding, while other regions are necessary for transmitting conformational changes through the protein.

The KCO binding and channel activation data, as well as structural models of SUR2A, led us to test a model[6] that, along with the previously identified regions that include the coupling helices and the MSD2-NBD2 linker, suggests the NBDs also form part of the KCO binding sites (Figure 1B, solid black circle). Thus, we have probed binding of two KCOs, pinacidil and diazoxide, to SUR2A NBD1, which along with coupling helix 3 and NBD2 may be involved in creating a drug binding site. These studies were enabled by the finding that SUR2A NBD1 could be expressed as a soluble and folded domain,[38] while SUR2A NBD2 could not. In this paper, we demonstrate direct and specific binding of pinacidil to SUR2A NBD1 in the presence of MgATP using nuclear magnetic resonance (NMR) spectroscopy and use intrinsic tryptophan fluorescence to determine the affinity of the drug/NBD1 interaction. The pinacidil/NBD1 interaction is weak, having a K_d value of 455 ± 37 μM, which is consistent with the hypothesis that NBD1 forms part of the drug binding site and the demonstration of the involvement of other regions of the SUR proteins in previous studies.[23,35−37] In contrast, interactions between SUR2A NBD1 and diazoxide were not observed under the same conditions. Using fluorescence nucleotide binding studies, we demonstrate that pinacidil increases the nucleotide binding affinity of SUR2A NBD1, providing further evidence for a direct interaction between pinacidil and NBD1. NMR relaxation experiments and size exclusion chromatography demonstrate that SUR2A NBD1 is monomeric under the conditions used in the drug binding studies. Together, these experiments identify an additional component of the binding site for pinacidil on SUR2A, which is likely at an interface between coupling helix 3 and NBD1 that forms part of the drug binding site in the intact K_{ATP} channel. The studies also provide a methodological approach for testing binding of drugs to the NBDs of the SUR proteins.

EXPERIMENTAL PROCEDURES

Materials. The K_{ATP} channel openers (KCOs) pinacidil and diazoxide were purchased from Sigma. The KCOs purchased were ≥98% pure according the manufacturer.

Protein Expression and Purification. NBD1 from rat SUR2A (residues S615-L933) was prepared as previously described.[38] The sequence of rat SUR2A is ∼96% identical to human SUR2A in this region, with most amino acid changes occurring in unstructured loops.[38] Thus, data acquired on rat SUR2A NBD1 is applicable to the human protein. Briefly, SUR2A NBD1 is expressed as a fusion with a cleavable N-terminal 6xHis-SUMO tag in *Eschericha coli* BL21 (DE3) CodonPlus-RIL (Stratagene) cells. Cells were grown in media containing 95% ^{15}N-labeled M9 minimal media and 5% LB media at 18 °C. The 6xHis-SUMO fusion protein was isolated using a Ni^{2+}-NTA affinity column (GE Healthcare). Following cleavage of the 6xHis-SUMO tag with His-Ulp1 protease, SUR2A NBD1 was purified to homogeneity by size exclusion chromatography (Superdex 75, GE Healthcare), followed by a reverse Ni^{2+}-NTA affinity column to remove small amounts of the 6xHis-SUMO tag that coelute with SUR2A NBD1 from the size exclusion column. All protein purification steps were conducted at 4 °C. For the NMR and fluorescence studies, SUR2A NBD1 was exchanged into NBD1 buffer (20 mM sodium phosphate pH 7.3, 150 mM NaCl, 2% (v/v) glycerol, 2 mM DTT) with and without ATP and $MgCl_2$, as required.

Homology Models. Homology models of rat SUR2A (Figure 1B) were generated with the program Modeler.[41] A structure-based sequence alignment (Supplementary Figure 1, Supporting Information) of the C-subfamily of ABC transporters,[12] including isoforms of SUR2,[42,43] based on available structural data of full[13−15] and half transporters (PDB code 4AYT) available was generated using Clustal W.[44,45] Structural information from the crystal structure of CFTR NBD1, which

dx.doi.org/10.1021/bi301019e | *Biochemistry* 2012, 51, 9211−9222

is similar to SUR2A NBD1[38] was also used in the alignment. The homology models were generated using the crystal structure of Sav1866 (PDB code 2HYD)[14] and the human CFTR F508A NBD1-RE (PDB code 1XMI),[46] excluding residues C647−D673, as templates. A total of 50 models were generated, from which the 10 lowest energy models were selected for analysis.

Drug Binding Studies by NMR Spectroscopy. Interaction of SUR2A NBD1 with K_{ATP} channel openers (KCOs) was monitored with NMR spectra of SUR2A NBD1. The purified SUR2A NBD1 was dialyzed into NBD1 buffer with 5 mM ATP and 5 mM $MgCl_2$. The NMR samples also contained 0.5 mM 4,4-dimethyl-4-silapentane-1-sulfonic acid (DSS) for ^1H and ^{15}N chemical shift referencing.[47] NMR drug binding studies were done with SUR2A NBD1 at a concentration of 250 μM. TROSY-HSQC spectra[48] of SUR2A NBD1 were recorded at 30 °C on a 600 MHz Varian Inova spectrometer equipped with a H(F)CN triple resonance cryoprobe and actively shielded z-gradients. The KCO drugs were solubilized in DMSO. Sequential additions of the drugs were made to the SUR2A NBD1 sample and NMR spectra were recorded. Three separate titrations were done with pinacidil and two with diazoxide, using different preparations of the protein. To account for changes in spectra of SUR2A NBD1 from addition of increasing amounts of DMSO, blank titrations of SUR2A NBD1 in which identical volumes of DMSO without the drug were recorded. Thus, the spectra of SUR2A NBD1 with and without drug shown have identical amounts of DMSO. All NMR data were processed using NMRPipe/NMRDraw[49] and analyzed using NMRView.[50] Spectra with and without the drug were compared by calculating the combined chemical shift difference, $\Delta\delta_{total}$, according to the equation, $\Delta\delta_{total} = ((W_{HN}\Delta\delta_{HN})^2 + (W_N\Delta\delta_N)^2)^{1/2}$,[51,52] where $\Delta\delta_{HN}$ and $\Delta\delta_N$ are the chemical shift differences in the ^1HN and ^{15}N dimensions, respectively. W_{HN} (1.55) and W_N (0.236)[53] are weighting factors determined from the spread in chemical shifts contained in the BMRB.[54]

We also recorded 1D-^1H spectra for each titration point in order to experimentally determine the drug and DMSO concentrations in solution at each point in the titration.[55] Addition of drug to the protein sample results in a dilution of the DMSO concentration, which compromises the solubility of the drug. Thus, the amount of drug in solution during the titration may not be equal to the amount of drug added due to precipitation. For pinacidil, we used resonances from the tertbutyl (0.93 ppm), methyl (1.18 ppm), and aromatic (7.19 and 8.35 ppm) protons (Supplementary Figure 2A). These signals were integrated and divided by the total number of protons (signal:proton ratio) that give rise to the signals. For diazoxide, we used resonances from the methyl (2.39 ppm), and aromatic (7.36, 7.73, 7.96 ppm) protons (Supplementary Figure 2B). For DMSO, we used the resonance from the methyl protons (2.72 ppm). The signal:proton ratio for each drug was compared to that for glycerol, for which we determine the concentration based on our starting concentration and the dilution in the titration, to obtain values for the concentration of drug and DMSO in our NMR titration samples. This method allows for determination of the free drug in solution, as resonances for drug bound to the protein would be broadened and/or overlapped with the protein resonances, and hence not observable in the 1D-^1H spectrum. The free drug concentrations at the end of the titration were determined to be in 10−15-fold molar excess compared with the protein concentration. Thus, the total concentration of drug is underestimated by <10%, even if we were to consider saturation of the protein with drug. We also prepared standard samples of pinacidil (Supplementary Figure 2A) and diazoxide (Supplementary Figure 2B), in which there was no precipitation of the drug, and verified the drug and DMSO concentrations by the same method. These calibration standards also verified the drug and DMSO concentrations in our titration samples. The 1D spectra were processed and analyzed with the ACD/NMR Processor (Academic Edition, version 12.1) software package (www.acdlabs.com).

Intrinsic Tryptophan Fluorescence Experiments. K_d values for the interaction of pinacidil and NBD1 in the presence of 5 mM MgATP were determined using intrinsic Trp fluorescence of the NBD1. Fluorescence experiments were conducted on a Fluoromax-4 spectrofluorimeter equipped with an automatic titrator and a Peltier unit for precise temperature control. Experiments were conducted at 15 °C, with excitation and emission wavelengths of 298 and 348 nm, respectively, and slit widths of 1.5 and 6 nm, respectively. The excitation wavelength of 298 nm was chosen to selectively excite Trp residues in the protein, and the emission wavelength of 348 nm corresponds to the wavelength where the fluorescence difference of NBD1 in the absence and presence of pinacidil NBD1 is at a maximum. The affinity between NBD1 and pinacidil was measured using 1 μM protein in NBD1 buffer containing 10% DMSO to ensure solubility of the drug at the highest concentrations used in the experiment (~ 1 mM). The titration data were fit to the equation,[56] assuming a 1:1 complex between NBD1 and the drug,

$$I = I_o + \frac{(I_\infty - I_o)}{2[\mathrm{NBD1}_{total}]}\{([\mathrm{KCO}_{total}] + [\mathrm{NBD1}_{total}] + K_d) - [([\mathrm{KCO}_{total}] + [\mathrm{NBD1}_{total}] + K_d)^2 - 4([\mathrm{KCO}_{total}])([\mathrm{NBD1}_{total}])]^{1/2}\}$$

where I is the fluorescence intensity at a given total concentration of pinacidil, $[KCO_{total}]$, I_∞ is the fluorescence intensity at saturation, I_o is the fluorescence intensity in absence of the drug, K_d is the dissociation constant, and $[NBD1_{total}]$ is the total concentration of SUR2A NBD1 in the reaction.

NMR Relaxation Experiments. ^{15}N $R_{1\rho}$ relaxation experiments were performed at 30 °C on a Varian Inova 600 MHz spectrometer equipped with an HCN triple-resonance cryoprobe with actively shielded z-gradients using previously published pulse schemes.[57,58] ^{15}N $R_{1\rho}$ values were measured from six different spectra recorded with delays of 2, 4, 8.5, 14, 21, and 30 ms for a sample of 250 μM NBD1 in the presence of saturating concentrations of MgATP. Relaxation experiments were not recorded in the presence of pinacidil due to limited solubility of the drug over the time required for the acquiring the relaxation data (~2 days). ^{15}N R_2 values for each residue were obtained by correction of the observed relaxation rate $R_{1\rho}$ for the offset $\Delta\nu$ of the applied spin-lock rf field (ν_1) to the resonance using the relation $R_{1\rho} = R_2 \sin^2\theta$, where $\theta = \tan^{-1}(\nu_1/\Delta\nu)$ and ν_1 was 1824 Hz. All data sets were processed using NMRPipe. Peak intensities were obtained using the Rate Analysis tool in NMRView and used to fit a two parameter function of the form $I(t) = I_0^{e-t*R2}$ using a Matlab script.[59] Errors in relaxation rates were estimated by Monte Carlo analysis. In total, 24 resolved peaks were analyzed.

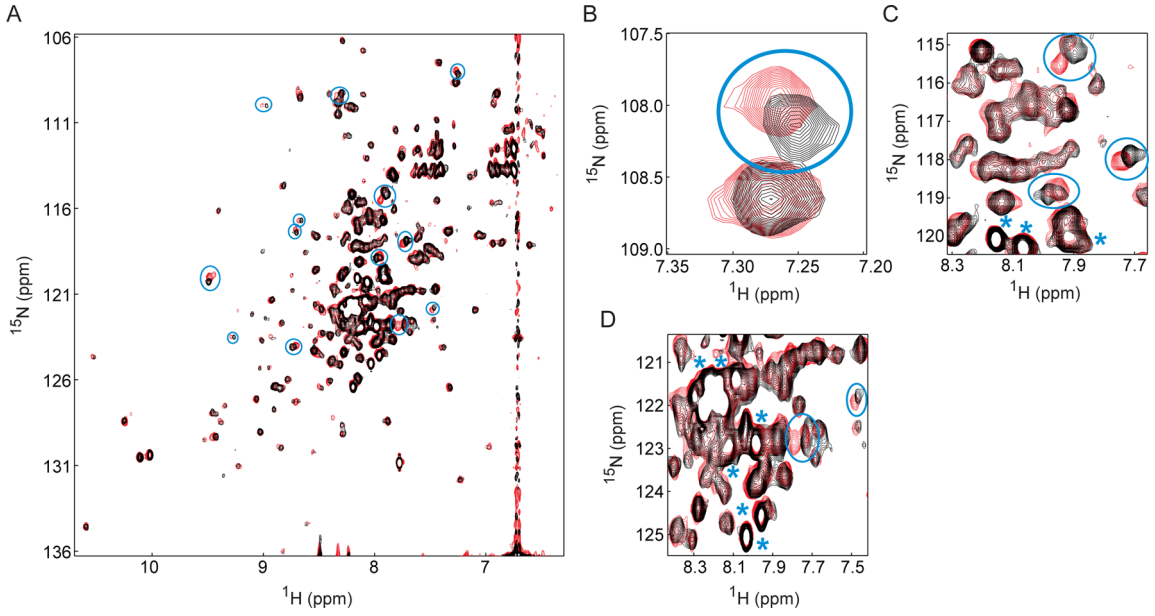

Figure 2. Pinacidil interacts with SUR2A NBD1 in the presence of MgATP. (A) Comparison of 2D ^{15}N−^{1}H TROSY-HSQC[48] spectra of SUR2A NBD1 (250 μM) in the absence and presence of 3.9 mM pinacidil with 5 mM Mg^{2+} and 5 mM ATP in 20 mM Na phosphate, pH 7.3, 150 mM NaCl, 5 mM DTT, 2% (v/v) glycerol, 7.5% (v/v) DMSO, 10% (v/v) D_2O at 30 °C at 600 MHz. Chemical shifts for each spectrum were referenced to 4,4-dimethyl-4-silapentane-1-sulfonic acid (DSS).[47] The spectrum of SUR2A NBD1 in the absence of pinacidil is in the foreground with resonances colored in black, while the spectrum of NBD1 with 3.9 mM pinacidil is in the background in red. Blue circles highlight specific chemical shift changes in NBD1 upon addition of pinacidil. (B−D) Selected regions of the spectrum shown in (A). As with panel A, blue circles highlight chemical shift changes observed with addition of pinacidil. The asterisks (" * ") in panels C and D identify some of the resonances from disordered regions in the protein.

Fluorescence Nucleotide Binding Experiments. K_d values for the interaction between SUR2A NBD1 (S615-L933) and the fluorescent ATP analogue 2′,3′-*O*-(2,4,6-trinitrophenyl)- adenosine-5′-triphosphate (TNP-ATP, Molecular Probes) were determined using fluorescence spectroscopy. These studies required removal of ATP present in the NBD1 samples from the purification. Mg^{2+} and ATP were removed from NBD1 samples by size exclusion chromatography and replaced with known concentrations (2.5 μM) of $MgCl_2$ and TNP-ATP. SUR2A NBD1 elutes from the size exclusion column (Superdex 75, GE Healthcare) at 10.7 mL, which is consistent with momomeric NBD1.[38] Binding experiments were performed by serial dilutions of the protein at a constant concentration of the fluorescent TNP-ATP. An initial sample containing 50−70 μM NBD1 (depending on the concentration of apo NBD1 that eluted from the size exclusion column), 2.5 μM TNP-ATP and 2.5 μM $MgCl_2$ in the NBD1 buffer with 10% (v/v) glycerol was generated. Samples with lower NBD1 concentrations were made by serial dilutions into buffer lacking the protein, while maintaining constant $MgCl_2$ and TNP-ATP concentrations. Thus samples ranged in protein concentration from 0.1−1 μM for the lowest NBD1 concentration to 50−70 μM NBD1, with constant Mg^{2+} and TNP-ATP concentrations of 2.5 μM. A separate sample was generated containing $MgCl_2$, TNP-ATP and buffer only for the 0 μM NBD1 sample. Because of lack of stability and solubility of apo NBD1, binding experiments were performed at 15 °C. Fluorescence spectra of TNP-ATP were recorded immediately after each sample was generated using an excitation wavelength of 465 nm and a slit width of 5 nm. Emission spectra were recorded from 485 nm to 600 nm with slit widths of 7 nm. The K_d value for the NBD1-nucleotide complex was determined by monitoring the ratio between the fluorescence intensity at 533 nm, which corresponds to the wavelength where fluorescence difference of free and bound TNP-ATP is at a maximum, and 600 nm to account for any nonspecific fluorescence from the protein.[60] The titration data were fit to the equation

$$I = I_o + \frac{(I_\infty - I_o)}{2[\mathrm{TNP}_{total}]}\{([\mathrm{TNP}_{total}] + [\mathrm{NBD1}_{total}] + K_d) - [([\mathrm{TNP}_{total}] + [\mathrm{NBD1}_{total}] + K_d)^2 - 4([\mathrm{TNP}_{total}])([\mathrm{NBD1}_{total}])]^{1/2}\}$$

where I is the fluorescence intensity ratio at a given total concentration of TNP-ATP, $[\mathrm{TNP}_{total}]$, I_∞ is the fluorescence intensity ratio at saturation, I_o is the fluorescence intensity ratio in absence of ligand, K_d is the dissociation constant, and $[\mathrm{NBD1}_{total}]$ is the total concentration of SUR2A NBD1 in the reaction. This equation assumes a 1:1 complex of NBD1 with TNP-ATP.[56,61]

We kept the TNP-ATP concentrations constant as described previously,[61,62] rather than the protein concentration as done in other studies[63,64] because of the lack of stability of apo SUR2A NBD1 over time. By employing serial dilutions, we measured the fluorescence of samples with excess NBD1 before any precipitation occurred. To determine the effects of pinacidil and diazoxide on nucleotide binding, the TNP-ATP binding experiments were performed in the presence of 12.5 μM pinacidil or diazoxide. A concentration of 12.5 μM of drugs was chosen, rather than 50 μM, which is equal to the highest concentration of NBD1 in the titration, because pinacidil has a weak fluorescent signal when excited at 465 nm. The fluorescence of pinacidil at 12.5 μM is negligible.

dx.doi.org/10.1021/bi301019e | *Biochemistry* 2012, 51, 9211−9222

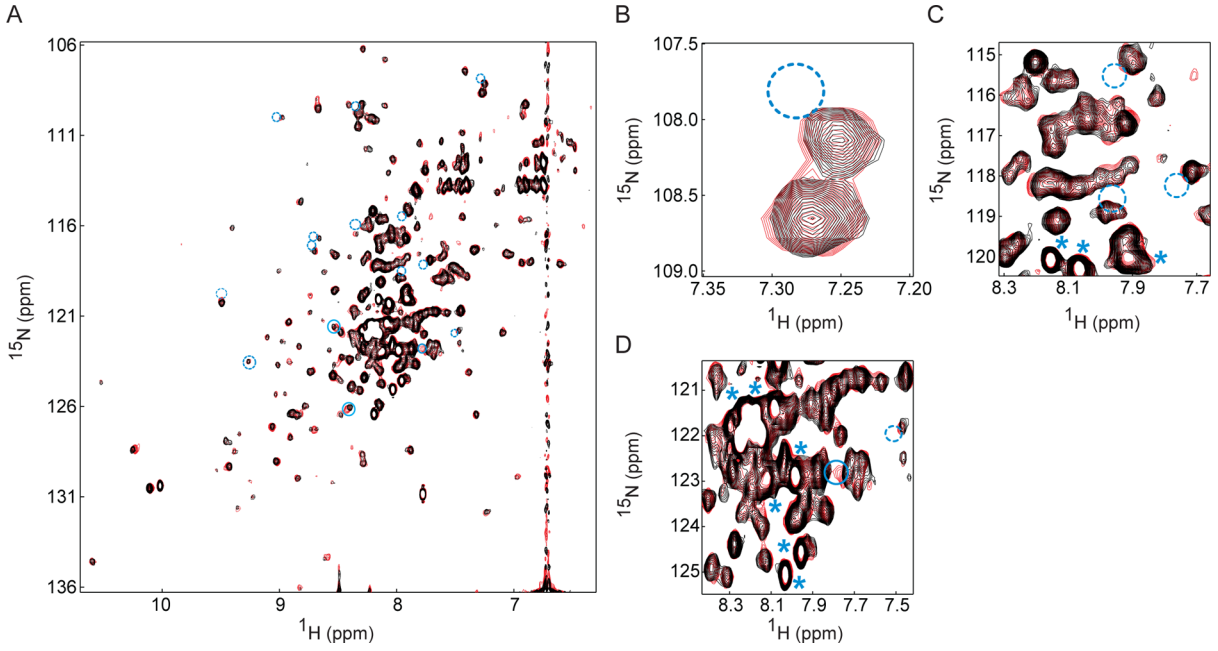

Figure 3. Diazoxide does not interact with SUR2A NBD1 in the presence of MgATP. (A) Comparison of 2D ^{15}N–^{1}H TROSY-HSQC[48] spectra of SUR2A NBD1 (250 μM) in the absence and presence of 3.8 mM diazoxide at 30 °C at 600 MHz. The solution conditions for each sample are identical to those described in the legend to Figure 2. The spectrum of SUR2A NBD1 in the absence of diazoxide is in the foreground with resonances colored in black, while that of NBD1 with diazoxide is in the background with resonances colored red. Spectra of SUR2A NBD1 with and without diazoxide are virtually identical. Minor chemical shift changes, which are seen for only two resonances and only with high (3.8 mM) concentrations of diazoxide, are circled (blue, solid). Dashed blue circles highlight resonances for which significant chemical shift changes are seen with pinacidil addition (Figure 2), but which are absent in the diazoxide titration. (B–D) Selected regions of the spectrum shown in panel A. The resonance circled in panel D by a solid blue circle shows small chemical shift changes ($\Delta\delta_{total} < 0.03$). The asterisks (" * ") identify resonances from disordered regions in the protein.

RESULTS

NMR Titration Studies Indicate That NBD1 of rSUR2A Mediates Specific Interactions with Pinacidil. ^{15}N TROSY-HSQC spectra of SUR2A NBD1 were recorded in the absence and presence of the drugs pinacidil (Figure 2) and diazoxide (Figure 3). As explained in the Experimental Procedures section, and as seen with other drugs used in NMR binding studies,[65] the pinacidil and diazoxide have poor solubility in the aqueous NBD1 buffer and hence are dissolved in DMSO. Thus, blank titrations of SUR2A NBD1 using only DMSO were also performed to account for changes in the SUR2A NBD1 spectra with increasing concentrations of DMSO (Supplementary Figure 3). Figures 2 and 3 comparing spectra in absence and presence of drugs were recorded with identical concentrations of DMSO (v/v, 7.5%).

Addition of pinacidil to SUR2A NBD1 results in 13 distinct chemical shift changes throughout spectra of SUR2A NBD1 (Figure 2), indicating that the KCO pinacidil interacts with SUR2A NBD1. The number and magnitude of the chemical shift changes are consistent with spectral changes seen upon binding of a small molecule drug to NBD1 of CFTR using similar concentrations of protein and drug.[65] Only resonances exhibiting a significant combined chemical shift difference, which is greater than the average of all $\Delta\delta_{total}$ values plus one standard deviation, $\Delta\delta_{total} \geq 0.04$,[66] are considered. Resonances displaying changes in intensity are not considered when analyzing spectral changes because decreases in intensity may be due to small amounts of protein precipitation during the titration. Further, overlapping resonances were also not considered in the analysis. The small number of chemical shift changes observed in NBD1 upon addition of pinacidil is expected due to the small size of the drug molecule and indicates that the drug interacts with specific residues in SUR2A NBD1.

Notably, all of the observed chemical shift changes occurred for resonances from structured residues in the protein. We do not observe chemical shift changes in the intense resonances centered about 8.2 ppm in the ^{1}H dimension (Figure 2C,D; marked with an " * ") that result from disordered regions in SUR2A NBD1, such as the disordered region of the β-sheet subdomain insert,[38] indicating that these regions in SUR2A NBD1 do not interact with pinacidil. Of the 13 resonances that exhibit chemical shift changes upon pinacidil addition, 9 resonances have ^{1}H chemical shifts of less than or equal to 7.7 ppm (i.e., 7.7, 7.5, and 7.3 ppm) and greater than 8.5 ppm (i.e., 8.6, 9.0, 9.3, 9.5, and two peaks at 8.7 ppm). Additional chemical shifts are seen for residues with ^{1}H chemical shifts of 7.8, 7.9, 8.0, and 8.3 ppm. The lower intensities of these resonances (Figure 2C,D; highlighted by cyan circles) compared to the intense resonances described above (Figure 2C,D; marked with an "*") suggest that they are also from structured residues in the protein. Although Figure 2 shows HSQC spectra taken with 0 mM pinacidil and 3.9 mM pinacidil (with DMSO concentrations (v/v) of 7.5%), chemical shift changes were observed with as little as 1.5 mM pinacidil added. These drug concentrations are of the same order of magnitude as the concentrations used to observe pinacidil-mediated activation of K_{ATP} channels in some electrophysiological studies[34,37,67] and were necessary here due to the high protein concentration needed for NMR spectroscopy. Spectra of NBD1 are similar with 2.4 mM and 3.9 mM pinacidil added to the sample (Supplementary Figure 4). None of the resonances

dx.doi.org/10.1021/bi301019e | *Biochemistry* 2012, 51, 9211–9222

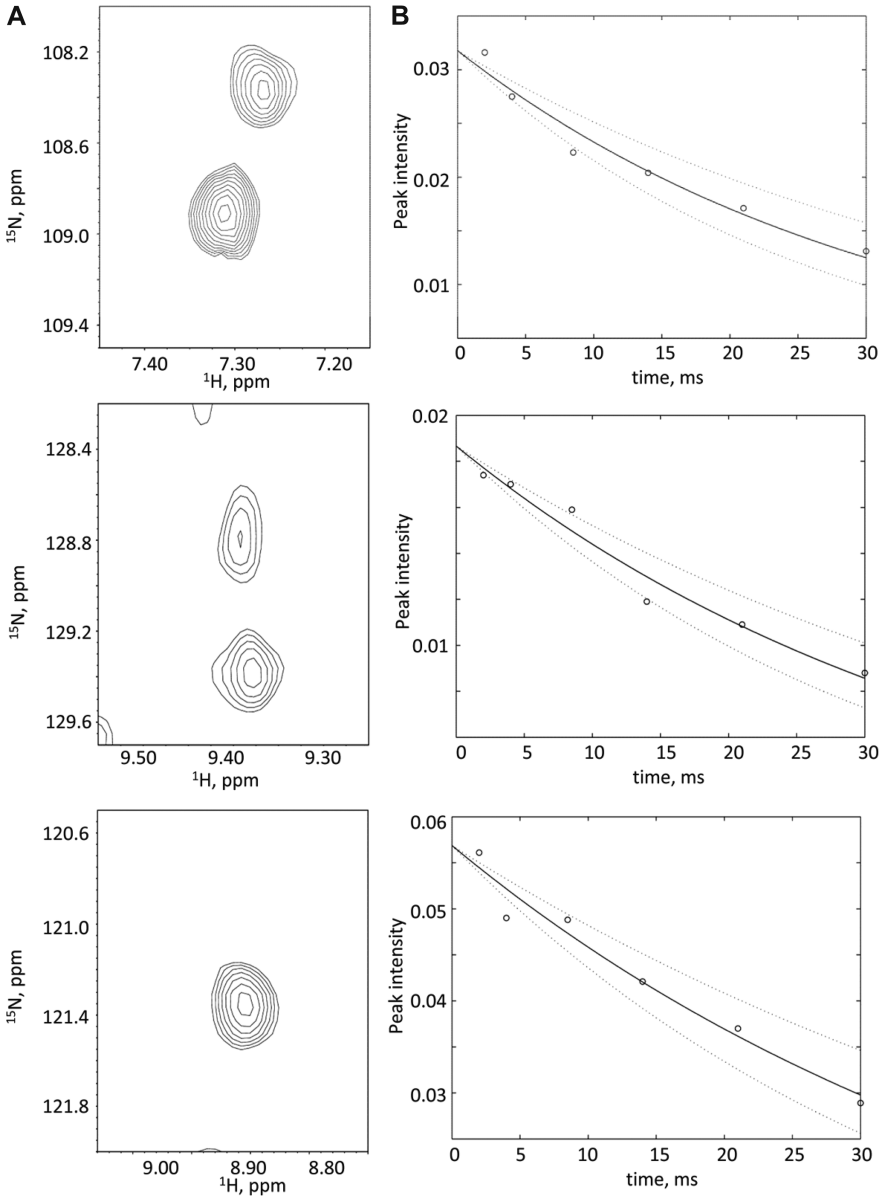

Figure 4. ^{15}N R_2 relaxation data for 250 μM SUR2A NBD1. (A) Selected regions from the ^{15}N-^{1}H correlation spectrum recorded with the pulse sequence used to determine ^{15}N $R_{1\rho}$ rates with a delay time of 2 ms. (B) Examples of ^{15}N $R_{1\rho}$ decay curves for peaks shown in (A). The ^{15}N $R_{1\rho}$ rates were used to determine ^{15}N R_2 rates, as described in the Experimental Procedures section.

display significant chemical shift changes ($\Delta\delta_{total}$ < 0.03 for all resonances) between the two spectra, indicating that 2.4 mM pinacidil is sufficient to reach saturation in the titration. Identification of the specific residues in SUR2A NBD1 that interact with pinacidil would require resonance assignment of the protein, which in turn requires concentrated samples of NBD1 (≥0.5 mM) to be stable for many days (>14 days) at 30 °C. We are currently developing strategies to allow for this series of extensive and involved experiments.

In contrast to pinacidil, diazoxide does not bind SUR2A NBD1, or at least binds too weakly to be detected by these experiments. Spectra of 250 μM SUR2A NBD1 in the absence and presence of 3.8 mM diazoxide, a 15-fold excess of the compound, are virtually identical (Figure 3). Only two resonances, out of 260 total, displayed a significant, but small difference in chemical shift ($\Delta\delta_{total}$ = 0.04) (Figure 3A, circled). There is also another resonance that may change with diazoxide addition (Figure 3D, circled), but the $\Delta\delta_{total}$ value calculated for this resonance is not statistically significant. In comparison, addition of pinacidil results in 13 resonances with significant $\Delta\delta_{total}$ values of 0.04−0.10. Many of the resonances that display chemical shift changes with pinacidil addition do not change with addition of diazoxide (Figure 2, solid circles compared to Figure 3, dashed circles). Thus, the NMR data indicate that pinacidil makes specific interactions with NBD1, while diazoxide does not interact with NBD1 or interacts with a much lower affinity than pinacidil. Spectra with higher concentrations of diazoxide to detect lower affinity interactions could not be recorded due to the solubility of the compound.

In the intact SUR2A protein, as with other ABC transporters, NBD1 and NBD2 form a heterodimer upon binding of MgATP.[17] We have recorded ^{15}N TROSY-HSQC spectra of SUR2A NBD1 at various concentrations (from 50 μM > 300 μM). SUR2A NBD1 elutes from the 24 mL Superdex 75 size exclusion chromatograph column at a volume of 10.7 mL, consistent with it being monomeric. Spectra of SUR2A NBD1

dx.doi.org/10.1021/bi301019e | *Biochemistry* 2012, 51, 9211−9222

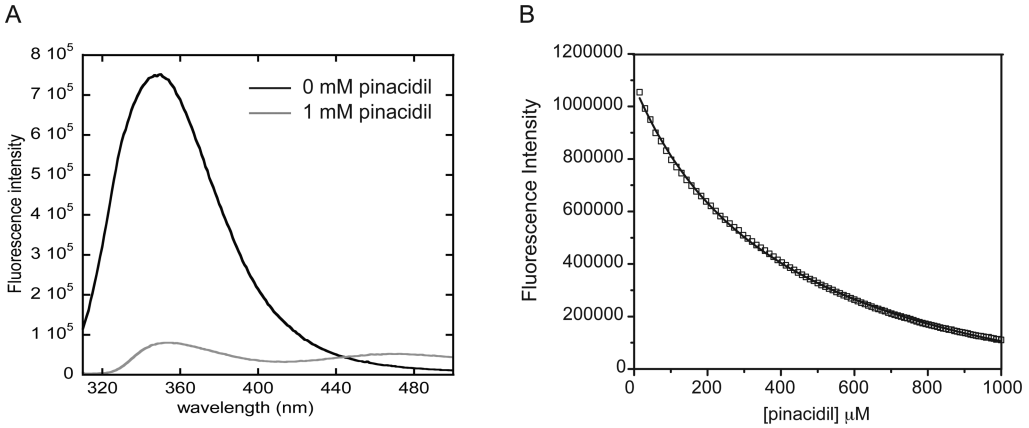

Figure 5. Binding of pinacidil to SUR2A NBD1 as monitored by intrinsic Trp fluorescence. (A) Emission spectra of 1 μM SUR2A NBD1 in the NBD1 buffer with 5 mM MgATP and 10% (v/v) DMSO in the absence (black line) and presence of 1 mM pinacidil (gray line). (B) Binding of pinacidil to SUR2A NBD1 as monitored by quenching of Trp fluorescence. The data (open squares) were fit assuming a 1:1 complex (solid line),[56,61] as described in the Experimental Procedures.

samples at 50 μM concentration, which are taken directly from the eluent (at 10.7 mL) of the size exclusion column without concentration of the sample further, are identical in peak positions, and relative intensities, also indicate that the samples of NBD1 up to 300 μM are monomeric.[38] The absence of dimerization of SUR2A NBD1 in the presence of MgATP is consistent with observations of NBDs from other eukaryotic ABC transporters, in which NBD1 and NBD2 are not identical, that demonstrate monomeric behavior of NBD1 even at the high concentrations used in structural studies.[46,66,68,69]

Further confirmation of momomeric SUR2A NBD1 in our samples comes from NMR ^{15}N R_2 relaxation studies. ^{15}N R_2 rates were calculated for 24 resonances, with resonances selected from regions of the spectrum that are derived from structured regions of the protein, such as those with ^{1}H chemical shifts of >8.5 ppm. Resonances with ^{1}H chemical shifts of 7.7−8.5 ppm were excluded because of potential overlap or partial overlap, which compromises analysis of relaxation data, in this region of the spectrum. A subset of decay curves from the ^{15}N $R_{1\rho}$ experiment, which are used to calculate the ^{15}N R_2 rates, is shown in Figure 4. The calculated ^{15}N R_2 rates for these resonances were used to calculate a correlation time (τ_m) for SUR2A NBD1 using only the J(0) term for the spectral density function and assuming an order parameter (S^2) of 0.85, which is the average S^2 value expected for a folded protein.[57] Only the J(0) term was considered because it dominates the ^{15}N R_2 relaxation of large molecules, such as proteins.[70] We calculate a correlation time of 25.3 ± 4.5 ns. This value compares favorably with an expected correlation time of 22 ns calculated for a homology model of SUR2A NBD1 from HYDRONMR,[71] indicating that our sample of SUR2A NBD1 is predominantly monomeric under these conditions.

Specific Binding of Pinacidil by SUR2A NBD1 Displays a Low Affinity. SUR2A NBD1 contains a total of six Trp residues that are located throughout the protein, that produce a large fluorescence signal (Figure 5A). Changes in the environment of one or more Trp residues from direct binding of pinacidil or conformational changes associated with binding have the potential to produce changes in Trp emission spectra in proteins.[60] SUR2A NBD1 displays a large fluorescence signal, owing to the six Trp residues in the protein. Indeed, addition of pinacidil results in a large quenching of Trp fluorescence (Figure 5A), indicating direct binding of pinacidil to NBD1. Quenching of fluorescence often results from exposure of Trp residues to the solvent, which in this case would suggest conformational changes upon pinacidil binding. However, quenching of fluorescence may also result in other situations. For example, direct binding of pinacidil to a site involving a Trp may cause quenching depending on the orientation of the aromatic group in pinacidil and a Trp residue in the protein. Quenching may occur because pinacidil binding causes conformational changes in NBD1 that bring acidic residues in close proximity to one or more Trp residues. Regardless of the quenching mechanism, the large changes in the fluorescence spectrum of NBD1 indicate an interaction with pinacidil. Although the spectra shown in Figure 5A are for 1 μM SUR2A NBD1 in the absence and presence of 1 mM pinacidil, a significant amount of quenching (~50%) is seen with much lower pinacidil concentrations (i.e., 100 μM). A K_d value of 455 ± 37 μM was obtained from pinacidil titration of SUR2A NBD1 (Figure 5B). The relatively low affinity interaction is likely because we are probing pinacidil binding to NBD1 alone and not in the presence of coupling helices, and therefore reflective of having only part of the pinacidil binding site present in the experiment.

Binding of Pinacidil Changes the Affinity of NBD1 for MgATP. After establishing that pinacidil binds SUR2A NBD1 by NMR and fluorescence spectroscopy, we used fluorescence spectroscopy to probe the effect of pinacidil on the nucleotide affinity of NBD1. Although previous work demonstrated the interaction of SUR2A NBD1 (S615-L933) with MgATP using NMR spectroscopy,[38] we could not use NMR titration experiments to determine the affinity of the interaction due to the tendency of the nucleotide-free NBD1 to precipitate at concentrations greater than 100 μM at 30 °C, which are the conditions necessary for the NMR experiments.

The interaction between SUR2A NBD1 and nucleotide was probed using the fluorescent ATP analogue TNP-ATP. TNP-ATP has a trinitrophenyl fluorophore on the ribose of the nucleotide and has been employed to study nucleotide binding to ATP binding proteins including kinases[61,62] and other ABC transporters, such as P-glycoprotein[63] and CFTR.[64] The affinities for ATP and ADP may[72] or may not[61] be different from that of their fluorescent analogues. Nonetheless, these probes have been used successfully to compare changes in

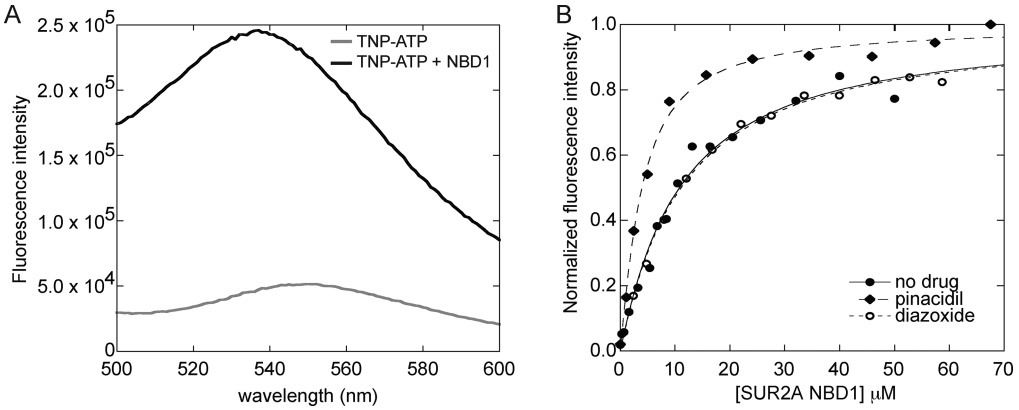

Figure 6. TNP-ATP binding SUR2A NBD1 in the absence and presence of pinacidil. (A) Emission spectra of 2.5 μM TNP-ATP in the NBD1 buffer in the absence (gray line) and presence of 50 μM SUR2A NBD1 (black line). (B) Binding of SUR2A NBD1 to TNP-ATP as monitored by increasing fluorescence of TNP-ATP. TNP-ATP fluorescence titration data acquired in the absence of drug are shown as solid circles and were fit assuming a 1:1 complex, shown by the solid line,[56,61] as described in the Experimental Procedures. Data from NBD1 titration of TNP-ATP acquired in the presence of pinacidil are shown as solid diamonds with the fit of the TNP-ATP titration data shown as a dashed line. The data and the fit from the TNP-ATP titration in the presence of diazoxide are shown as open circles and a dotted line, respectively. TNP-ATP titration data in the presence of pinacidil and diazoxide were fit assuming a 1:1 complex for the NBD1/nucleotide interaction.

nucleotide binding in other NBDs under different experimental conditions, such as in wild type and mutant states.[64,73,74]

Upon addition of SUR2A NBD1, the fluorescence emission spectra of TNP-ATP changes so that the intensity increases and the maximum is blue-shifted (Figure 6A), corresponding to the direct binding of TNP-ATP by NBD1. Addition of increasing amounts of NBD1 resulted in a concentration-dependent and saturable increase in TNP-ATP fluorescence (Figure 6B; closed circles, solid lines). The K_d value obtained from these measurements shows tight binding of NBD1 to TNP-ATP (8.0 μM ± 1.0 μM). A similar K_d value was obtained for the interaction of TNP-ATP with NBD1 from CFTR,[64] which is in the same subfamily of ABC proteins as SUR2A.[12]

In the presence of 12.5 μM pinacidil, NBD1 titration of TNP-ATP also displays a saturable fluorescence increase (Figure 6B; solid diamonds, dashed line). However, the K_d value for the interaction between TNP-ATP and pinacidil-bound NBD1 is decreased to 3.1 ± 0.5 μM. The increase in the affinity of NBD1 for TNP-ATP in the presence of 12.5 μM of pinacidil suggests that pinacidil stabilizes the interaction between the nucleotide and NBD1. Similar titration experiments were performed in the presence of diazoxide (Figure 6B; open circles, dotted line). In this case, no change in the affinity of NBD1 and TNP-ATP (K_d value = 11.8 ± 3.0 μM) was observed, consistent with the NMR data that did not demonstrate an interaction between diazoxide and SUR2A NBD1. The K_d values measured are shown in Table 1.

Table 1. Dissociation Constants for Interactions of SUR2A NBD1 with Nucleotide[a]

nucleotide	K_d (μM)
TNP-ATP	8.0 ± 1.0 (3)
TNP-ATP (in the presence of pinacidil)	3.1 ± 0.5 (3)
TNP-ATP (in the presence of diazoxide)	11.9 ± 3.0 (2)

[a]The equilibrium dissociation constants (K_d, μM) were determined using fluorescence of the trinitrophenyl moiety of TNP-ATP and are reported as averages ± standard deviations. The number in parentheses indicates number of experiments performed for each binding analysis.

DISCUSSION

The data in this paper demonstrate, for the first time, a direct interaction of the KCO pinacidil with SUR2A NBD1. ^{15}N R_2 relaxation experiments and other lines of evidence[38] presented suggest that the NBD1 is not an artificial homodimer, even at the high concentrations of protein and nucleotide used in these experiments. We currently do not have resonance assignments for the protein, and therefore cannot specifically identify NBD1 residues that interact with pinacidil. However, the NMR titration data show chemical shift changes for a number of resonances from structured regions in the protein upon addition of pinacidil. The intense resonances, which are derived from disordered regions in NBD1 such as the β-sheet subdomain insert and C-terminal extension,[38] do not exhibit chemical shift changes upon pinacidil addition. The number and magnitude of the spectral shift changes are consistent with an interaction of pinacidil with specific residues in NBD1.[65] The observation that many of the resonances in the NBD1 spectrum do not change upon addition of pinacidil demonstrate that binding of pinacidil does not cause gross changes to the protein structure. Further, quenching of Trp fluorescence in NBD1 upon addition of pinacidil and the finding that binding of pinacidil to NBD1 increases the affinity of NBD1 for nucleotide also demonstrate a direct interaction between pinacidil and NBD1. Previous work has demonstrated the involvement of residues in coupling helix 3,[36] the MSD2-NBD2 linker,[36] TM helix 17,[37] and the C42 region[23] in binding of pinacidil and/or mediation of its effects in the intact K_{ATP} channel. Structures of ABC proteins[13−15] and our homology model of SUR2A revealed that coupling helix 3 forms an interface with NBD1 and NBD2, and that the flexible linker can also interact at this site. Therefore, the data we present here on the interaction of pinacidil with NBD1 is consistent with earlier studies that sought to localize the binding site of pinacidil in the intact SUR2A. Of note, there is a Trp residue, Trp 756, at this interface. Although changes in fluorescence can be due to multiple mechanisms, quenching of the fluorescence of Trp756 may occur due to direct binding of pinacidil at this site. Together with residues in coupling helix 3,[36] the MSD2-NBD1 linker,[36] and NBD2, residues around Trp 756 in NBD1 may be involved in pinacidil binding. The relatively low affinity that we

dx.doi.org/10.1021/bi301019e | Biochemistry 2012, 51, 9211−9222

measured for the binding of isolated NBD1 with pinacidil is consistent with the hypothesis that NBD1 contributes only part of the pinacidil binding site in the intact channel, with the full binding site comprised of residues from the coupling helices and the MSD2-NBD1 linker,[6,36] and residues of NBD1 and NBD2.

In contrast to pinacidil, the NMR data indicate that diazoxide does not bind SUR2A NBD1, as indicated by other studies.[34,35] Earlier studies demonstrated that, in general, diazoxide can activate SUR1-containing K_{ATP} channels, but not SUR2A-containing channels.[6,26,28,29] Notably, diazoxide sensitivity can be conferred to SUR2A-containing K_{ATP} channels by transfer of MSD1-NBD1 from SUR1 to SUR2A,[35] indicating that SUR2A NBD1 is not involved in the diazoxide binding interface in SUR2A, consistent with the lack of interaction between diazoxide and SUR2A NBD1 observed here. Further, while residues L1249 and T1253 in SUR2A are involved in pinacidil activation, mutation of the corresponding residues in SUR1 has no affect on diazoxide-mediated activation of SUR1-containing channels.[37] These studies indicate that separate regions mediate the effect of diazoxide and other openers, such as pinacidil.[34]

Residues involved in KCO binding are not necessarily involved in K_{ATP} channel activation. Chimeras between SUR2A and MRP1 indicated that residues E1305, I1310, and L1313 are important for channel activation by, but not binding[67] of, the pinacidil analogue P1075. Residue E1305 is located in the MSD2-NBD2 linker and residues I1310 and L1313 are located in NBD2. Recent structures of ABC proteins[13−15] and our SUR2A homology model show that the MSD2-NBD2 linker contacts coupling helix 3, which in turn contacts NBD1. Thus, interaction of coupling helix 3 with pinacidil could affect the conformation of residues in the MSD2-NBD2 linker and in NBD2, such as E1305, I1310, and L1313, leading to changes in channel activation, possibly by coupling to Kir6.2.[67,75]

Conformational changes and dynamics are important to link KCO binding to channel activation. Conformational changes are expected in the NBDs from ATP binding and hydrolysis during the gating cycle. Drug binding may enhance these functionally relevant conformational changes. For example, increases in nucleotide binding to NBD1 in intact K_{ATP} channels, as we observed for the isolated SUR2A NBD1, in the presence of pinacidil may enhance structural and dynamic changes required for channel gating. A similar effect has been demonstrated in a recent study showing enhanced conformational changes in CFTR NBD1 upon drug binding that are comparable to the structural changes involved in gating of the CFTR channel.[65] Further drug binding studies encompassing different regions of the K_{ATP} channel, such as SUR2A NBD2, as well as different KCOs, may elucidate some of these mechanisms.

■ ASSOCIATED CONTENT

Supporting Information

Supporting Information includes a structure-based sequence alignment of SUR2A used to generate the homology model shown in Figure 1B, 1D−^{1}H NMR spectra of pinacidil and diazoxide, 2D ^{15}N−^{1}H TROSY-HSQC spectra of SUR2A in the NBD1 buffer with and without DMSO, and 2D ^{15}N−^{1}H TROSY-HSQC spectra of SUR2A with different concentrations of pinacidil. This material is available free of charge via the Internet at http://pubs.acs.org.

■ AUTHOR INFORMATION

Corresponding Author

*Tel: 1-905-569-4542; fax: 1-905-828-5425; e-mail: voula.kanelis@utoronto.ca.

Funding

This work was funded by grants from the Canadian Institutes of Health Research (CIHR) (MOP-106470) and the Natural Sciences and Engineering Council of Canada (RGPIN 357118-09) to V.K. V.K. is supported by a Early Researcher Award and CIHR New Investigator Award. J.P.L.-A. is supported by an Ontario Postdoctoral Fellowship and E.D.A. is supported by a Queen Elizabeth II Graduate Scholarship in Science and Technology.

Notes

The authors declare no competing financial interest.

■ ACKNOWLEDGMENTS

We thank John L. Rubinstein and Ronald A. Venters for critically reading the manuscript and for useful discussions. We acknowledge Ranjith Muhandiram for acquisition of ^{15}N NMR relaxation data and thank Lewis E. Kay for very helpful discussions.

■ ABBREVIATIONS USED

K_{ATP} channel, ATP-sensitive potassium channel; SUR, sulfonylurea receptor; ATP, adenosine triphosphate; ADP, adenosine diphosphate; NBD, nucleotide binding domain; KCO, K_{ATP} channel opener; NMR, nuclear magnetic resonance; MSD, membrane spanning domain; TM, transmembrane helix; C42 region, the C-terminal 42 residues in SUR proteins; SUMO, small ubiquitin-like modifier; DTT, dithiothreitol; DSS, 4,4-dimethyl-4-silapentane-1-sulfonic acid; TROSY, transverse relaxation optimized spectroscopy; HSQC, heteronuclear single quantum coherence; TNP-ATP, 2′,3′-*O*-(2,4,6-trinitrophenyl)-adenosine-5′-triphosphate

■ REFERENCES

(1) Seino, S., and Miki, T. (2003) Physiological and pathophysiological roles of ATP-sensitive K+ channels. *Prog. Biophys. Mol. Biol. 81*, 133−176.

(2) Nichols, C. G. (2006) K_{ATP} channels as molecular sensors of cellular metabolism. *Nature 440*, 470−476.

(3) Kane, G. C., Liu, X. K., Yamada, S., Olson, T. M., and Terzic, A. (2005) Cardiac K_{ATP} channels in health and disease. *J. Mol. Cell. Cardiol. 38*, 937−943.

(4) Jahangir, A., and Terzic, A. (2005) K(ATP) channel therapeutics at the bedside. *J. Mol. Cell. Cardiol. 39*, 99−112.

(5) Mikhailov, M. V., Campbell, J. D., de Wet, H., Shimomura, K., Zadek, B., Collins, R. F., Sansom, M. S., Ford, R. C., and Ashcroft, F. M. (2005) 3-D structural and functional characterization of the purified K_{ATP} channel complex Kir6.2-SUR1. *EMBO J. 24*, 4166−4175.

(6) Ashcroft, F. M., and Gribble, F. M. (2000) New windows on the mechanism of action of K(ATP) channel openers. *Trends Pharmacol. Sci. 21*, 439−445.

(7) Ashcroft, F. M., and Gribble, F. M. (2000) Tissue-specific effects of sulfonylureas: lessons from studies of cloned K(ATP) channels. *J. Diabetes Complications 14*, 192−196.

(8) Schwappach, B., Zerangue, N., Jan, Y. N., and Jan, L. Y. (2000) Molecular basis for K(ATP) assembly: transmembrane interactions mediate association of a K+ channel with an ABC transporter. *Neuron 26*, 155−167.

(9) Masia, R., Enkvetchakul, D., and Nichols, C. G. (2005) Differential nucleotide regulation of K_{ATP} channels by SUR1 and SUR2A. *J. Mol. Cell. Cardiol. 39*, 491−501.

(10) Matsuoka, T., Matsushita, K., Katayama, Y., Fujita, A., Inageda, K., Tanemoto, M., Inanobe, A., Yamashita, S., Matsuzawa, Y., and Kurachi, Y. (2000) C-terminal tails of sulfonylurea receptors control ADP-induced activation and diazoxide modulation of ATP-sensitive K(+) channels. *Circ. Res. 87*, 873−880.
(11) Solbach, T. F., Konig, J., Fromm, M. F., and Zolk, O. (2006) ATP-binding cassette transporters in the heart. *Trends Cardiovasc. Med. 16*, 7−15.
(12) Dean, M., Rzhetsky, A., and Allikmets, R. (2001) The human ATP-binding cassette (ABC) transporter superfamily. *Genome Res. 11*, 1156−1166.
(13) Aller, S. G., Yu, J., Ward, A., Weng, Y., Chittaboina, S., Zhuo, R., Harrell, P. M., Trinh, Y. T., Zhang, Q., Urbatsch, I. L., and Chang, G. (2009) Structure of P-glycoprotein reveals a molecular basis for poly-specific drug binding. *Science 323*, 1718−1722.
(14) Dawson, R. J., and Locher, K. P. (2006) Structure of a bacterial multidrug ABC transporter. *Nature 443*, 180−185.
(15) Ward, A., Reyes, C. L., Yu, J., Roth, C. B., and Chang, G. (2007) Flexibility in the ABC transporter MsbA: Alternating access with a twist. *Proc. Natl. Acad. Sci. U. S. A. 104*, 19005−19010.
(16) Hollenstein, K., Dawson, R. J., and Locher, K. P. (2007) Structure and mechanism of ABC transporter proteins. *Curr. Opin. Struct. Biol. 17*, 412−418.
(17) Higgins, C. F., and Linton, K. J. (2004) The ATP switch model for ABC transporters. *Nat. Struct. Mol. Biol. 11*, 918−926.
(18) Babenko, A. P., and Bryan, J. (2002) SUR-dependent modulation of K_{ATP} channels by an N-terminal KIR6.2 peptide. Defining intersubunit gating interactions. *J. Biol. Chem. 277*, 43997−44004.
(19) Babenko, A. P., and Bryan, J. (2003) Sur domains that associate with and gate K_{ATP} pores define a novel gatekeeper. *J. Biol. Chem. 278*, 41577−41580.
(20) Bryan, J., Vila-Carriles, W. H., Zhao, G., Babenko, A. P., and Aguilar-Bryan, L. (2004) Toward linking structure with function in ATP-sensitive K+ channels. *Diabetes 53* (Suppl 3), S104−112.
(21) Fang, K., Csanady, L., and Chan, K. W. (2006) The N-terminal transmembrane domain (TMD0) and a cytosolic linker (L0) of sulphonylurea receptor define the unique intrinsic gating of K_{ATP} channels. *J. Physiol. 576*, 379−389.
(22) Zingman, L. V., Alekseev, A. E., Bienengraeber, M., Hodgson, D., Karger, A. B., Dzeja, P. P., and Terzic, A. (2001) Signaling in channel/enzyme multimers: ATPase transitions in SUR module gate ATP-sensitive K+ conductance. *Neuron 31*, 233−245.
(23) Schwanstecher, M., Sieverding, C., Dorschner, H., Gross, I., Aguilar-Bryan, L., Schwanstecher, C., and Bryan, J. (1998) Potassium channel openers require ATP to bind to and act through sulfonylurea receptors. *EMBO J. 17*, 5529−5535.
(24) Gomma, A. H., Purcell, H. J., and Fox, K. M. (2001) Potassium channel openers in myocardial ischaemia: therapeutic potential of nicorandil. *Drugs 61*, 1705−1710.
(25) Pollesello, P., and Mebazaa, A. (2004) ATP-dependent potassium channels as a key target for the treatment of myocardial and vascular dysfunction. *Curr. Opin. Crit. Care 10*, 436−441.
(26) Moreau, C., Prost, A. L., Derand, R., and Vivaudou, M. (2005) SUR, ABC proteins targeted by K_{ATP} channel openers. *J. Mol. Cell. Cardiol. 38*, 951−963.
(27) Ashcroft, F. M., and Rorsman, P. (1989) Electrophysiology of the pancreatic beta-cell. *Prog. Biophys. Mol. Biol. 54*, 87−143.
(28) Flagg, T. P., Kurata, H. T., Masia, R., Caputa, G., Magnuson, M. A., Lefer, D. J., Coetzee, W. A., and Nichols, C. G. (2008) Differential structure of atrial and ventricular K_{ATP}: atrial KATP channels require SUR1. *Circ. Res. 103*, 1458−1465.
(29) Glukhov, A. V., Flagg, T. P., Fedorov, V. V., Efimov, I. R., and Nichols, C. G. (2010) Differential K(ATP) channel pharmacology in intact mouse heart. *J. Mol. Cell. Cardiol. 48*, 152−160.
(30) Isomoto, S., and Kurachi, Y. (1997) Function, regulation, pharmacology, and molecular structure of ATP-sensitive K+ channels in the cardiovascular system. *J. Cardiovasc. Electrophysiol. 8*, 1431−1446.
(31) Terzic, A., Jahangir, A., and Kurachi, Y. (1995) Cardiac ATP-sensitive K+ channels: regulation by intracellular nucleotides and K+ channel-opening drugs. *Am. J. Physiol. 269*, C525−545.
(32) Wheeler, A., Wang, C., Yang, K., Fang, K., Davis, K., Styer, A. M., Mirshahi, U., Moreau, C., Revilloud, J., Vivaudou, M., Liu, S., Mirshahi, T., and Chan, K. W. (2008) Coassembly of different sulfonylurea receptor subtypes extends the phenotypic diversity of ATP-sensitive potassium (K_{ATP}) channels. *Mol. Pharmacol. 74*, 1333−1344.
(33) Quayle, J. M., Nelson, M. T., and Standen, N. B. (1997) ATP-sensitive and inwardly rectifying potassium channels in smooth muscle. *Physiol. Rev. 77*, 1165−1232.
(34) D'Hahan, N., Moreau, C., Prost, A. L., Jacquet, H., Alekseev, A. E., Terzic, A., and Vivaudou, M. (1999) Pharmacological plasticity of cardiac ATP-sensitive potassium channels toward diazoxide revealed by ADP. *Proc. Natl. Acad. Sci. U. S. A. 96*, 12162−12167.
(35) Babenko, A. P., Gonzalez, G., and Bryan, J. (2000) Pharmaco-topology of sulfonylurea receptors. Separate domains of the regulatory subunits of K(ATP) channel isoforms are required for selective interaction with K(+) channel openers. *J. Biol. Chem. 275*, 717−720.
(36) Uhde, I., Toman, A., Gross, I., Schwanstecher, C., and Schwanstecher, M. (1999) Identification of the potassium channel opener site on sulfonylurea receptors. *J. Biol. Chem. 274*, 28079−28082.
(37) Moreau, C., Jacquet, H., Prost, A. L., D'Hahan, N., and Vivaudou, M. (2000) The molecular basis of the specificity of action of K(ATP) channel openers. *EMBO J. 19*, 6644−6651.
(38) De Araujo, E. D., Ikeda, L. K., Tzvetkova, S., and Kanelis, V. (2011) The First Nucleotide Binding Domain of the Sulfonylurea Receptor 2A Contains Regulatory Elements and Is Folded and Functions as an Independent Module. *Biochemistry 50*, 6655−6666.
(39) Matsushita, K., Kinoshita, K., Matsuoka, T., Fujita, A., Fujikado, T., Tano, Y., Nakamura, H., and Kurachi, Y. (2002) Intramolecular interaction of SUR2 subtypes for intracellular ADP-Induced differential control of K(ATP) channels. *Circ. Res. 90*, 554−561.
(40) Hung, L. W., Wang, I. X., Nikaido, K., Liu, P. Q., Ames, G. F., and Kim, S. H. (1998) Crystal structure of the ATP-binding subunit of an ABC transporter. *Nature 396*, 703−707.
(41) Sali, A., and Blundell, T. L. (1993) Comparative protein modelling by satisfaction of spatial restraints. *J. Mol. Biol. 234*, 779−815.
(42) Chutkow, W. A., Makielski, J. C., Nelson, D. J., Burant, C. F., and Fan, Z. (1999) Alternative splicing of SUR2 exon 17 regulates nucleotide sensitivity of the ATP-sensitive potassium channel. *J. Biol. Chem. 274*, 13656−13665.
(43) Chutkow, W. A., Simon, M. C., Le Beau, M. M., and Burant, C. F. (1996) Cloning, tissue expression, and chromosomal localization of SUR2, the putative drug-binding subunit of cardiac, skeletal muscle, and vascular K_{ATP} channels. *Diabetes 45*, 1439−1445.
(44) Larkin, M. A., Blackshields, G., Brown, N. P., Chenna, R., McGettigan, P. A., McWilliam, H., Valentin, F., Wallace, I. M., Wilm, A., Lopez, R., Thompson, J. D., Gibson, T. J., and Higgins, D. G. (2007) Clustal W and Clustal X version 2.0. *Bioinformatics 23*, 2947−2948.
(45) Thompson, J. D., Higgins, D. G., and Gibson, T. J. (1994) CLUSTAL W: improving the sensitivity of progressive multiple sequence alignment through sequence weighting, position-specific gap penalties and weight matrix choice. *Nucleic Acids Res. 22*, 4673−4680.
(46) Lewis, H. A., Zhao, X., Wang, C., Sauder, J. M., Rooney, I., Noland, B. W., Lorimer, D., Kearins, M. C., Conners, K., Condon, B., Maloney, P. C., Guggino, W. B., Hunt, J. F., and Emtage, S. (2005) Impact of the deltaF508 mutation in first nucleotide-binding domain of human cystic fibrosis transmembrane conductance regulator on domain folding and structure. *J. Biol. Chem. 280*, 1346−1353.
(47) Wishart, D. S., Bigam, C. G., Yao, J., Abildgaard, F., Dyson, H. J., Oldfield, E., Markley, J. L., and Sykes, B. D. (1995) ^{1}H, ^{13}C and ^{15}N chemical shift referencing in biomolecular NMR. *J. Biomol. NMR 6*, 135−140.

(48) Pervushin, K., Riek, R., Wider, G., and Wuthrich, K. (1997) Attenuated T_2 relaxation by mutual cancellation of dipole-dipole coupling and chemical shift anisotropy indicates an avenue to NMR structures of very large biological macromolecules in solution. *Proc. Natl. Acad. Sci. U. S. A. 94*, 12366−12371.
(49) Delaglio, F., Grzesiek, S., Vuister, G. W., Zhu, G., Pfeifer, J., and Bax, A. (1995) NMRPipe: a multidimensional spectral processing system based on UNIX pipes. *J. Biomol. NMR 6*, 277−293.
(50) Johnson, B. A., and Blevins, R. A. (1994) NMRView: a computer program for the visualization and analysis of NMR data. *J. Biomol. NMR 4*, 603−614.
(51) Ayed, A., Mulder, F. A., Yi, G. S., Lu, Y., Kay, L. E., and Arrowsmith, C. H. (2001) Latent and active p53 are identical in conformation. *Nat. Struct. Biol. 8*, 756−760.
(52) Mulder, F. A., Schipper, D., Bott, R., and Boelens, R. (1999) Altered flexibility in the substrate-binding site of related native and engineered high-alkaline Bacillus subtilisins. *J. Mol. Biol. 292*, 111−123.
(53) Schumann, F. H., Riepl, H., Maurer, T., Gronwald, W., Neidig, K. P., and Kalbitzer, H. R. (2007) Combined chemical shift changes and amino acid specific chemical shift mapping of protein-protein interactions. *J. Biomol. NMR 39*, 275−289.
(54) Seavey, B. R., Farr, E. A., Westler, W. M., and Markley, J. L. (1991) A relational database for sequence-specific protein NMR data. *J. Biomol. NMR 1*, 217−236.
(55) Pauli, G. F., Godecke, T., Jaki, B. U., and Lankin, D. C. (2012) Quantitative (1)h NMR. Development and potential of an analytical method: an update. *J. Nat. Prod. 75*, 834−851.
(56) Viguera, A. R., Arrondo, J. L., Musacchio, A., Saraste, M., and Serrano, L. (1994) Characterization of the interaction of natural proline-rich peptides with five different SH3 domains. *Biochemistry 33*, 10925−10933.
(57) Farrow, N. A., Muhandiram, R., Singer, A. U., Pascal, S. M., Kay, C. M., Gish, G., Shoelson, S. E., Pawson, T., Forman-Kay, J. D., and Kay, L. E. (1994) Backbone dynamics of a free and phosphopeptide-complexed Src homology 2 domain studied by ^{15}N NMR relaxation. *Biochemistry 33*, 5984−6003.
(58) Korzhnev, D. M., Skrynnikov, N. R., Millet, O., Torchia, D. A., and Kay, L. E. (2002) An NMR experiment for the accurate measurement of heteronuclear spin-lock relaxation rates. *J. Am. Chem. Soc. 124*, 10743−10753.
(59) Finerty, P. J., Jr., Mittermaier, A. K., Muhandiram, R., Kay, L. E., and Forman-Kay, J. D. (2005) NMR dynamics-derived insights into the binding properties of a peptide interacting with an SH2 domain. *Biochemistry 44*, 694−703.
(60) Pain, R. H. (2005) Determining the fluorescence spectrum of a protein, *Curr. Protoc. Protein Sci.* Chapter 7, Unit 7 7.
(61) Guarnieri, M. T., Blagg, B. S., and Zhao, R. (2011) A high-throughput TNP-ATP displacement assay for screening inhibitors of ATP-binding in bacterial histidine kinases. *Assay Drug. Dev. Technol. 9*, 174−183.
(62) Vas, M., Merli, A., and Rossi, G. L. (1994) Antagonistic binding of substrates to 3-phosphoglycerate kinase monitored by the fluorescent analogue 2′(3′)-O-(2,4,6-trinitrophenyl)adenosine 5′-triphosphate. *Biochem. J. 301* (Pt 3), 885−891.
(63) Liu, R., and Sharom, F. J. (1997) Fluorescence studies on the nucleotide binding domains of the P-glycoprotein multidrug transporter. *Biochemistry 36*, 2836−2843.
(64) Rabeh, W. M., Bossard, F., Xu, H., Okiyoneda, T., Bagdany, M., Mulvihill, C. M., Du, K., di Bernardo, S., Liu, Y., Konermann, L., Roldan, A., and Lukacs, G. L. (2012) Correction of both NBD1 energetics and domain interface is required to restore DeltaF508 CFTR folding and function. *Cell 148*, 150−163.
(65) Hudson, R. P., Chong, P. A., Prostasevich, I. I., Vernon, R., Noy, E., Bihler, H., An, J. L., Kaild, O., Sela-Culang, I., Mense, M., Senderowitz, H., Brouillette, C. G., and Forman-Kay, J. D. (2012) Conformational Changes Relevant to Channel Activity and Folding within the first Nucleotide Binding Domain of CFTR. *J. Biol. Chem. 287*, 28480−28494.
(66) Kanelis, V., Hudson, R. P., Thibodeau, P. H., Thomas, P. J., and Forman-Kay, J. D. (2010) NMR evidence for differential phosphorylation-dependent interactions in WT and DeltaF508 CFTR. *EMBO J. 29*, 263−277.
(67) Dupuis, J. P., Revilloud, J., Moreau, C. J., and Vivaudou, M. (2008) Three C-terminal residues from the sulphonylurea receptor contribute to the functional coupling between the K(ATP) channel subunits SUR2A and Kir6.2. *J. Physiol. 586*, 3075−3085.
(68) Lewis, H. A., Buchanan, S. G., Burley, S. K., Conners, K., Dickey, M., Dorwart, M., Fowler, R., Gao, X., Guggino, W. B., Hendrickson, W. A., Hunt, J. F., Kearins, M. C., Lorimer, D., Maloney, P. C., Post, K. W., Rajashankar, K. R., Rutter, M. E., Sauder, J. M., Shriver, S., Thibodeau, P. H., Thomas, P. J., Zhang, M., Zhao, X., and Emtage, S. (2004) Structure of nucleotide-binding domain 1 of the cystic fibrosis transmembrane conductance regulator. *EMBO J. 23*, 282−293.
(69) Ramaen, O., Leulliot, N., Sizun, C., Ulryck, N., Pamlard, O., Lallemand, J. Y., Tilbeurgh, H., and Jacquet, E. (2006) Structure of the human multidrug resistance protein 1 nucleotide binding domain 1 bound to Mg2+/ATP reveals a non-productive catalytic site. *J. Mol. Biol. 359*, 940−949.
(70) Farrow, N. A., Zhang, O., Forman-Kay, J. D., and Kay, L. E. (1995) Comparison of the backbone dynamics of a folded and an unfolded SH3 domain existing in equilibrium in aqueous buffer. *Biochemistry 34*, 868−878.
(71) Garcia de la Torre, J., Huertas, M. L., and Carrasco, B. (2000) HYDRONMR: prediction of NMR relaxation of globular proteins from atomic-level structures and hydrodynamic calculations. *J. Magn. Reson. 147*, 138−146.
(72) Thomas, P. J., Shenbagamurthi, P., Ysern, X., and Pedersen, P. L. (1991) Cystic fibrosis transmembrane conductance regulator: nucleotide binding to a synthetic peptide. *Science 251*, 555−557.
(73) Grycova, L., Lansky, Z., Friedlova, E., Vlachova, V., Kubala, M., Obsilova, V., Obsil, T., and Teisinger, J. (2007) ATP binding site on the C-terminus of the vanilloid receptor. *Arch. Biochem. Biophys. 465*, 389−398.
(74) Logan, J., Hiestand, D., Daram, P., Huang, Z., Muccio, D. D., Hartman, J., Haley, B., Cook, W. J., and Sorscher, E. J. (1994) Cystic fibrosis transmembrane conductance regulator mutations that disrupt nucleotide binding. *J. Clin. Invest. 94*, 228−236.
(75) Rainbow, R. D., James, M., Hudman, D., Al Johi, M., Singh, H., Watson, P. J., Ashmole, I., Davies, N. W., Lodwick, D., and Norman, R. I. (2004) Proximal C-terminal domain of sulphonylurea receptor 2A interacts with pore-forming Kir6 subunits in K_{ATP} channels. *Biochem. J. 379*, 173−181.
(76) Antcliff, J. F., Haider, S., Proks, P., Sansom, M. S., and Ashcroft, F. M. (2005) Functional analysis of a structural model of the ATP-binding site of the K_{ATP} channel Kir6.2 subunit. *EMBO J. 24*, 229−239.
(77) Chan, K. W., Zhang, H., and Logothetis, D. E. (2003) N-terminal transmembrane domain of the SUR controls trafficking and gating of Kir6 channel subunits. *EMBO J. 22*, 3833−3843.